BACHELOR THESIS / BIOMEDICAL ENGINEERING 2022

Evaluation of the influence of cartilage endplates composition gradient on intervertebral disc degeneration

Raquel Andrés Abad

upf. Universitat Pompeu Fabra Barcelona

Evaluation of the influence of cartilage endplates composition gradient on intervertebral disc degeneration

Raquel Andrés Abad

Bachelor's thesis UPF 2022/2023

Thesis supervisor:

Dr. Carlos Ruiz Wills , (BCN MedTech - Biomechanics and Mechanobiology)

Acknowledgments

First and foremost, I would first like to thank my supervisor Carlos Ruiz Wills for giving me the opportunity of developing my thesis with him. Without his excellent guidance and assistance throughout the whole project, the present work would not have been possible. I also want to thank my fellow students, for brightening up every meeting and helping each other.

Second, I warmly thank my friends for both sharing the university experience and for building lifetime friendship.

I would also like to thank my family for their patience and continuous support in the distance throughout these years of study. If I ever lost the interest, you kept me motivated.

Abstract

Intervertebral disc (IVD) degeneration is one of the leading causes of Low Back Pain (LBP), a main cause of disability affecting 7.5% of global population. IVD degeneration has been directly related to alterations in the nutrition of the IVD. The main nutrition pathways are diffusion through the cartilage endplates (CEPs) and the capillaries surrounding the disc rim. Nevertheless, the role of the CEPs in IVD degeneration is unclear.

Experimental models showed a change in composition through the CEP, influencing its biochemical and transport properties. Numerical models can complement these results addressing the study of IVD degeneration. A previous 2D study showed that CEP gradient of permeability had influence in the mass exchange, however, the exploration of the influence of such gradient in a 3D model remains unexplored.

Hence, the aim of this project is to study the influence of CEP composition gradient on IVD degeneration using a 3D Finite Element IVD mechano-transport model. Two composition gradients were used, defined on a 2-layer CEP and a 4-layer CEP of elements, in two conditions Grade I (GI) and Grade III (GIII) of degeneration. On the one hand, fluid velocity and mass flow were studied by simulating a daily cycle activity. On the other hand, solutes concentrations and cell viability were explored during three days. Results showed a reduction in 24.60% of mass flow at the boundary CEP-Nucleus when using CEP composition gradient on GI and 11.98% on GIII. Glucose concentration decreased 29.76% and 8.40% on GI and GIII, respectively, inducing cell death at the anterior zone of the disc. The results suggest that it is important to consider the CEP composition gradient as it might act as a barrier in the solutes transport. Next step would be to implement the gradient on a patient-specific IVD cohort for better understanding IVD degeneration. Such knowledge might contribute to generate personalised treatment to enhance the quality of life of patient with LBP.

Keywords

Low Back Pain, intervertebral disc degeneration, disc nutrition, cartilage endplate, composition gradient

Preface

The subject for this bachelor thesis, raised from my interest on finding solutions to daily aches and pains. Intervertebral disc degeneration is a common clinical condition directly associated to Low Back Pain as one of its leading causes, with a prevalence of around 75%. This disease is caused by ageing and structural damage and it can be accelerated by lifestyle and health factors.

I have had the opportunity to develop my project on the Biomechanics and Mechanobiology (BMMB) department of BCN MedTech. The research of BMMB is focused on the load-bearing organs and tissues of the human body in health and disease. Their main research areas are: the spine and the intervertebral disc, the cartilage and its relation to osteoarthritis, bone and osteoporosis, motion analysis and body function.

I am presenting you the result 9 months of work, which allowed me to deepen my knowledge in biomechanics, mechanobiology and intervertebral disc degeneration. The final outcome of this project, although being in a premature stage, concludes that it highly relevant to include the CEP composition gradient of the IVD on 3D numerical models. This initial study will give a step to develop a more accurate 3D IVD model with the aim of improving diagnostic and treatment tools of an expanded disease such as intervertebral disc degeneration.

Index

List of Figures

List of Tables

1. INTRODUCTION

1.1 Problem and motivation

Low Back Pain (LBP) is a very common disorder and a costly medical condition. It is a leading cause of disability and one of the most common causes for visits to the medical doctor. The point prevalence of LBP in 2017 was estimated to be about 7.5% of the global population, or around 577 million people. It may imply a total cost between 0.1-2% of gross domestic product in European countries [1]. The low back supports the weight of the upper body and provides mobility for everyday motions such as bending and twisting. Injury to the muscles, ligaments, joints or lumbar intervertebral discs may result in low back pain, being lumbar intervertebral disc (IVD) degeneration one of the leading causes of the disorder [2].

IVD degeneration is a common condition caused by aging or structural damage. Its effects can be accelerated by injury, health and lifestyle factors and by genetic predisposition to joint pain or musculoskeletal disorders. Nearly everyone's discs degenerates over time, but not everyone feels pain. Unfortunately, the degenerative process cannot be reversed once it has started. Because of this, the current treatments against IVD degeneration aim at improving the health of the surrounding structures of the disc, such as the spinal nerves, vertebral bones and joints, and supporting muscles and ligaments [3].

The intervertebral disc is the largest avascular tissue of the human body, so its nutrition is one of the keys for staying healthy. Nutrients mainly arrive to the IVD by diffusion through the cartilage endplate (CEP) and outer rim of the annulus fibrosus [4]. Thus, changes in CEP composition may affect the diffusion of nutrients through it, altering the nutritional pathway of the IVD and, which may result in IVD degeneration [5] .

Over the last decades, a large number of experimental and computational studies have been developed [5,6,7,8,9,10]. The main aims are finding the causes and possible treatment strategies for intervertebral disc degeneration and also increasing the understanding of the processes involved in it [11,12,13,14]. Many of the studies are focused on the relation between disc nutrition and intervertebral disc degeneration. *In vitro* studies have shown that IVD cell growth and survival are associated with cell density and the availability of serum or nutrients [15].

Furthermore, *in vivo* studies through Magnetic Resonance Imaging (MRI) have demonstrated that the structure and mechanics of the CEP affects solute transport and disc mechanics [6]. Indeed, there is a chemical composition gradient through the CEP that may also affect the characteristics mentioned above [7,8].

At the same time, *in-silico* models have also been used. They are a powerful tool that helps in the understanding of the results of *in vivo* and *in vitro* experiments and reduces the need for expensive clinical trials with animal models, decreasing the time. In concrete, Finite Element Method (FEM) is one of the most used numerical technique, as it allows easier modeling of complex geometrical and irregular shapes and it can be adapted to meet specifications for accomplishing a high degree of accuracy.

Several 3D Finite Element IVD models have confirmed that a reduced nutrient supply at the cartilage endplates affects cell viability [9]. However, none of the studies performed to date considers the CEP composition gradient in a 3D IVD model. A recent study considered this CEP composition gradient on a 2D model. It showed its effect on mass fluid transport towards the Bony Endplate, but no implementation was made on a 3D model.

1.2 Aim

The aim of this project is to evaluate the influence of the cartilage endplate gradient of composition on disc nutrition using a 3D intervertebral disc mechano-transport model. Two Finite Element IVD models will be designed in order to study this influence through two different gradients of composition of the CEP. This study will also evaluate the differences between IVD models with different degradation grades, Grade I (GI) and Grade III (GIII).

2. STATE OF THE ART

2.1 The Spine

The Spine provides the main support for the body, allowing a person to stand upright, bend and twist. It is made up by the vertebrae, facet joints, intervertebral discs, spinal cords and nerves, and soft tissues, such as ligaments, muscles and tendons. The 33 vertebrae define five distinct spine segments. From the neck, they are: the cervical spine, the thoracic spine, the lumbar spine, the sacrum and the coccyx (Figure 1).

The lumbar spine consists of 5 vertebrae, classified by levels from 1 to 5 (L1-L5). They are the largest vertebrae of the whole spine, as they support and stabilize all the upper body. Between them, there is the intervertebral disc, five in total, which allows flexibility and provides protection from jarring movements together with the surrounding soft tissues. [16].

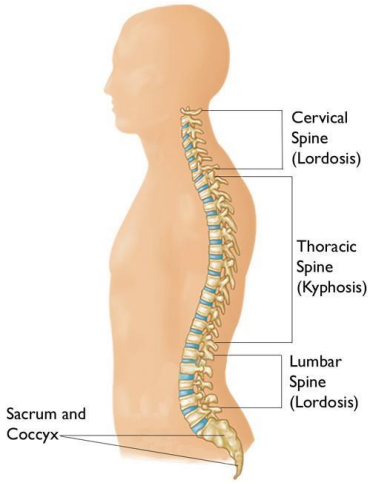

Figure 1. The Spine

2.2 The intervertebral disc

The intervertebral discs are the principal joint between two vertebrae in the spinal column. Their main/major function is mechanical. They provide flexibility to the spine, allowing bending, flexion and torsion, and a shock-absorbing effect as they are constantly transmitting loads arising from body weight and muscle activity through the spinal column. Indeed, they prevent the vertebrae from grinding together and protect the spinal cord and nerve roots. The intervertebral disc is also the largest avascular tissue in the body, undergoing more extensive changes with age and degeneration than any other tissue.

Anatomically, the IVD is a cushion of fibrocartilage which consists of three distinct anatomical regions: the nucleus pulposus (NP), the annulus fibrosus (AF), the transition zone (TZ) between these two and the cartilage endplates (Figure 2). They are mainly composed by water, proteoglycans and collagen in different proportions. Its height is between 7 mm and 10mm and it has a diameter of around 4 cm in the lumbar region of the spine. [7].

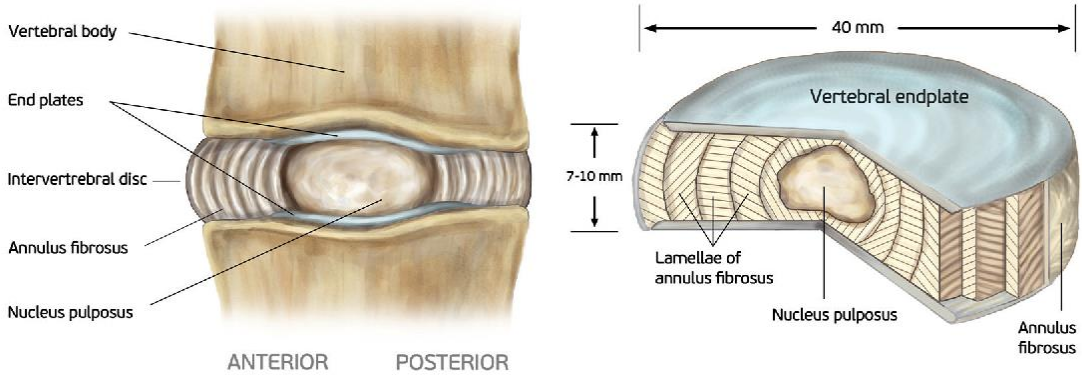

Figure 2. The intervertebral disc and its regions

2.2.1 Nucleus Pulposus

The nucleus pulposus is the soft inner core of the disc. It exerts a swelling pressure that allows the disc to withstand the spine compressive forces and to maintain disc height. The NP contains collagen and elastin fibers which are organized randomly and radially, respectively. These fibers are embedded in a highly hydrated matrix with proteoglycans. As proteoglycans are negatively charged, water molecules are retained within the nucleus through local osmotic effects giving the NP its swelling capacity.

2.2.2 Annulus Fibrosus

The peripheral and fibrocartilaginous annulus fibrosus consists of concentrically lamellated collagen fibers surrounding the NP. The collagen fibers of each lamella lie parallel. They are oriented at an angle of approximately 30-42º to the vertical axis and in opposite directions in successive layers. Between the lamellae there are elastin fibers.

This characteristic organization of the fibers within the annulus gives the IVD its anisotropic mechanical behavior.

2.2.3 Transition Zone

The transition zone is the region around the boundary between the nucleus and the annulus. Its composition is characteristic, as it does not follow the annulus' nor the nucleus' biosynthesis. It has been seen that it contains higher proteoglycan and protein biosynthesis than its surrounding tissues [17].

2.2.4 Cartilage Endplate

The cartilaginous endplates are two thin horizontal layers of less than 1 mm thick which, superiorly and inferiorly, confine the NP and the inner AF. The composition of this tissue is similar to that of hyaline cartilage, which is characterized by a high proteoglycan and collagen II content. The collagen fibers, predominantly collagen type II fibers, lie horizontal and parallel to the vertebral bodies. The cartilage endplates act as a mechanical barrier, they partially distribute the pressure absorbed by discs during loading and as a physical barrier, they help to prevent the nucleus bulging into the spongiosa of the vertebral bodies. In addition to this, the high permeability suggests that the CEP acts as a gateway for nutrient transport into disc, it allows the transport of fluid, nutrients waste products to the cells in the nucleus pulposus and part of the annulus fibrosus.

2.3 Disc nutrition

The intervertebral disc is the largest avascular tissue of the human body. Nutrients and the metabolite exchange come from the vascular network in the adjacent tissues (Figure 3). The main route for disc nutrition is the capillaries that arise in the vertebral bodies, penetrate the bony endplate and terminate at the bone-disc junction, the cartilage endplate. At this point, nutrients and waste products diffuse under gradients a total distance of 7-8mm to reach the nucleus and inner annulus cells for maintaining their cell viability and metabolic activity. These gradients depend on the rate of transport through the tissue to the cells and the rate of cellular demand. The secondary route for disc nutrition for the outer annulus cells is the capillaries in the soft tissues that surround the sides of the disc. [18, 5].

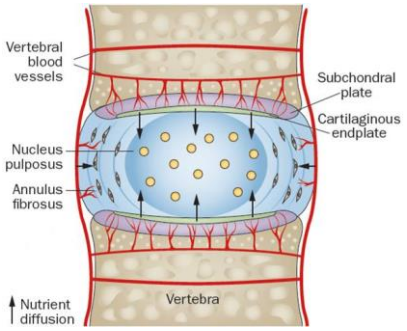

Figure 3. Blood supply to the intervertebral disc

2.4 Intervertebral disc degeneration

Intervertebral disc degeneration is a very common clinical condition directly implicated as a causative factor of low back pain. This disease is most common in older adults. Nevertheless, almost everyone has some disc degeneration after age 40, even if symptoms are not developed. It is due to ageing, structural damage and alterations in cell nutrition. The degeneration can be accelerated by injury, lifestyle factors and by genetic predisposition to joint pain or musculoskeletal disorders. It implies the loss of water content and disc height, resulting in pain and the loss of mobility of the body as the disc shrinks and dehydrates. [19]

A reduction in essential nutrients is thought to drive the progression of degeneration. It has been demonstrated that the structural features, mechanical and transport properties of the cartilage endplate play a role in disc nutrition [11,12]. The cartilage matrix must contain sufficient pore space to allow nutrient and metabolite transport to and from the avascular disc. This pore space depends on the osmotic swelling pressure and on the relative concentration of proteoglycans and collagen.

In addition to this, in 1989 it was shown that there is a change in composition through the cartilage endplate, being able to affect the permeability and transport properties of the structure [7]. Although it is a long time since this was discovered, its relation to intervertebral disc degeneration is understudied.

2.5 Intervertebral disc degeneration degree scale

Intervertebral disc degeneration is usually evaluated using the Standard Pfirrmann Grading Scale [20]. It assesses degenerated intervertebral discs by MRI for the asymmetry in disc structure, the distinction of the nucleus and the annulus, the signal intensity of intervertebral discs and the height of intervertebral discs. It assigns grade I to V for disc degeneration (Figure 4).

Grade I refers to a homogeneous disc with bright hyperintense white signal intensity and normal disc heigh, 0.7mm. Grade II refers to an inhomogeneous disc but keeping the hyperintense white signal. The NP and AF are clearly differentiated and disc height is normal. Grade III refers to an inhomogeneous disc with an intermittent gray signal intensity. The distinction between the NP and AF is unclear and disc height is normal or slightly decreased. Grade IV refers to an inhomogeneous disc with a hypointense dark gray signal intensity. There is no more distinction between the NP and AF and disc height is slightly or moderately decreased. Grade V refers to an inhomogeneous disc with a hypointense black signal intensity. Ther is no more difference between the NP and AF. The disc space is collapsed.

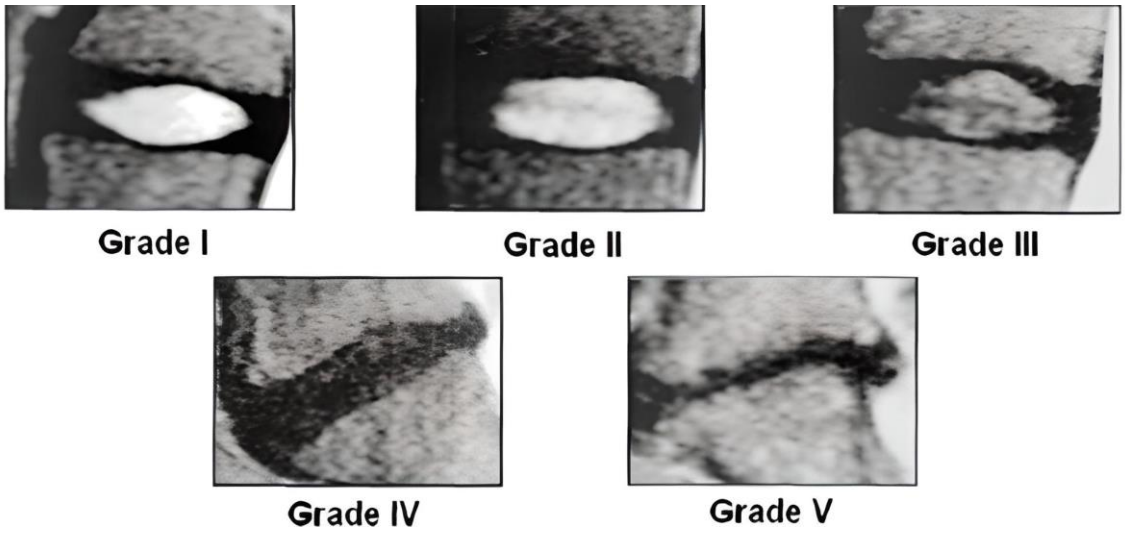

Figure 4. Grades of degeneration according to Pfirmann grading scale

2.6 Strategies to study disc degeneration

2.6.1 In vivo and in vitro experiments

Roberts et al [7] published the first evidence about the biochemical and structural properties of the CEP. The results of the chemical analyses performed showed a change in composition through the cartilage endplate, having higher collagen but lower proteoglycan and water contents at the outer annulus and nearer the bone than at the region of the endplate nearest the disc at the nucleus.

In the last years, new techniques have been introduced in order to study CEP morphology and thickness, such as MRI FLASH imaging [8]. The results obtained with this technique agree with previous literature, providing a new tool for non-invasive assessment and quantification of disc health. Despite its relevance, few computational studies have been developed considering the gradient in composition of the CEP.

Furthermore, experimental studies have demonstrated that transport properties of the cartilage endplate vary depending on the composition and calcification. Proteoglycans are key in regulating the movement of solutes into and out of the disc. It has been shown that the removal of proteoglycans from the endplate accelerates the loss of proteoglycans from the nucleus. Additionally, the more hydrated the matrix, the higher the degree of penetration and the more easily solutes could move. Having the opposite effect with the other components of the matrix [13]. Wong et Al. [12] demonstrated that physiologic fluctuations in human CEP composition and transport properties directly affect NP cells survival. They showed that CEPs with poor permeability appeared to have lower proteoglycans, collagen and significantly shorter viable distance from the CEP/nutrient interface. They associated solute diffusivity in the CEP with biochemical composition: low-diffusivity CEPs had greater amounts of collagen and proteoglycans, more mineral and lower cross-link maturity. Apart from this, there are studies that show how matrix modification enhances the transport properties of the CEP to improve disc nutrition [12].

Over again, all these results clearly reinforce the need for developing more computational studies focused on the influence of CEP composition on intervertebral disc degeneration.

2.6.2. In silico experiments: Finite Element models

There are few *in silico* experiments focused on the relation of cartilage endplates to intervertebral disc degeneration and there are even fewer studies focused on the cartilage endplates composition gradient.

Malandrino et al [9] demonstrated that a reduced nutrient supply at the endplates affected cell viability, interacting with tissue deformation. He simulated compressive daily cycles on a 3D intervertebral disc FE mechano-transport model, with constant composition of the CEP.

Ruiz Wills et Al. [10] evaluated how moderate CEP composition changes related to tissue degeneration can affect disc nutrition and cell viability. He developed a 2D Finite Element model of the central plug of the IVD, from the bony endplate (BEP) up to the IVD center. As for the CEP, the model considered a gradient of composition from the NP to the BEP, including a new CEP composition permeability approach. In addition to this, they created a 3D Finite Element model, but without considering a gradient of composition of the CEP. Thus, the influence of the cartilage endplate composition gradient on a 3D IVD model remains still unknown.

3. MATERIALS AND METHODS

3.1 Finite Element IVD model

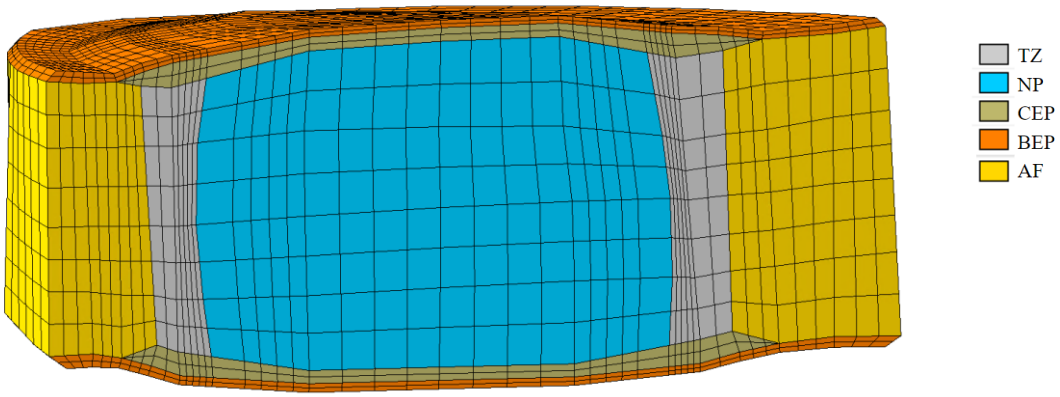

Figure 5. Generic 3D L4-L5 FE IVD model

A generic L4-L5 3D Finite Element IVD model was used (Figure 5) [10]. It was an axisymmetric, composition-based, mechano-transport model. The regions included were the annulus fibrosus (AF), the nucleus pulposus (NP), their transition zone (TZ), the cartilage endplates and the bony endplates. All disc tissues were considered as osmo-poro-visco-hyperelastic materials. Their formulation represents a relation between a swelling pressure stress which simulates the Donnan osmotic effects, a hyperelastic porous matrix saturated by intra and extra-fibrillar fluid and the viscoelastic collagen fibers, which are only present in the AF. The total stress tensor, σ, (Equation 1) is defined by the effective stress of the porous solid skeleton, σ_{eff}, (Equation 2) and a pore pressure component, p, (Equation 3) [21].

$$\sigma = \sigma_{eff} - p\boldsymbol{I} \qquad (1)$$

$$\boldsymbol{\sigma_{eff}} = -\frac{1}{6}\frac{\boldsymbol{Ln(J)}}{\boldsymbol{J}}\boldsymbol{G_m I}\left[-\mathbf{1} + \frac{\mathbf{3}(\boldsymbol{J}+\boldsymbol{n_{s,0}})}{(-\boldsymbol{J}+\boldsymbol{n_{s,0}})} + \frac{\mathbf{3JLn(J)}\boldsymbol{n_{s,0}}}{(-\boldsymbol{J}+\boldsymbol{n_{s,0}})^{\mathbf{2}}}\right] + \frac{\boldsymbol{G_m}}{\boldsymbol{J}}\left(\boldsymbol{B} - \boldsymbol{J}^{\frac{\mathbf{2}}{\mathbf{3}}}\boldsymbol{I}\right) \qquad (2)$$

$$p = u_w + \Delta\pi \qquad (3)$$

The pore pressure is the sum of the water chemical potential, u_w, and a swelling pressure term, $\Delta\pi$, (Equation 4) which depended on proteoglycan extra-fibrillar fixed charge density content ($C_{F,exf}$) between others [21].$C_{F,exf}$ expression (Equation 5) depended on extra-fibrillar water (n_{exf}) and normal fixed charge density (C_F) which represents proteoglycans content.

$$\Delta\boldsymbol{\pi} = \boldsymbol{\Phi_{int}RT}\left(\sqrt{\boldsymbol{C_{F,exf}^2} + \mathbf{4}\left(\frac{\boldsymbol{\gamma_{ext}^{\pm}}}{\boldsymbol{\gamma_{int}^{\pm}}}\right)^{\mathbf{2}}\boldsymbol{C_{ext}^2}}\right) - \mathbf{2}\boldsymbol{\Phi_{ext}RTC_{ext}} \qquad (4)$$

$$C_{F,exf} = \frac{n_f C_f}{n_{exf}} \qquad (5)$$

Collagen fibers, only present in the AF layers as reinforcement fibers, were considered as a viscoelastic material. The Bony Endplate (BEP), included in the model as a top and bottom layer for performing the simulations, was considered as a linear poroelastic material [14,20]. The material properties of the generic IVD model were the same as in Ruiz Wills et al. [10]. Table 1 shows the material properties of NP, AF and the CEP of constant composition. Material properties of collagen fibers and BEP are specified in 8.1 from Additional Information Section.

Tissue	Initial Water Content (%)		Initial Fixed Charge Density (mEq/ml)		Collagen Density (%)	
	Grade I	Grade III	Grade I	Grade III	Grade I	Grade III
AF	75	70	0,2	0,2	65	78
NP	80	76	0,3	0,23	15	28,5
CEP	66	60	0,17	0,13	24	35

Table 1. Material properties used

This composition-based model was coupled through tissue deformations and interstitial fluid flow to a transport model developed by Malandrino et al. [9]. This model considered the diffusion-reaction of oxygen, lactate and glucose (see 8.2 from Additional Information). The effective diffusivity of each solute was related to the solute diffusivity in water D_{water} and water content, n_f (Equation 6).

$$\boldsymbol{D_{solute}} = \left(\frac{\boldsymbol{n_f}}{\boldsymbol{2-n_f}}\right)^{\boldsymbol{2}} \boldsymbol{D_{water}} \boldsymbol{I} \qquad (6)$$

pH of the medium was calculated following Equation 7 [2] where it is directly related to lactate concentration. A is constant that quantifies the change of pH per unit of lactate concentration. It has a value of -1/11.11 nmol/mL.

$$\boldsymbol{pH} = 7.4 + A.C_{lact} \qquad (7)$$

Cell viability was considered as the ratio of cell density change over time over the initial cell density before any cell death occurs (Equation 8). Cell density, $\rho_{cell,}$ was defined as in Equation 9.

$$\text{Cell viability} = \boldsymbol{\rho_{cell}} / \boldsymbol{\rho_{cell,0}} \qquad (8)$$

$$\boldsymbol{\rho_{cell}} = \boldsymbol{\rho_{cell,0}} \boldsymbol{exp}(-\boldsymbol{\alpha_i t}) \qquad (9)$$

3.2 Modelling CEP composition gradient in 3D

The CEP of the generic L4-L5 FE IVD model was composed by a two-layer endplate of elements. It was adapted to the model of the four-layer endplate by a division by two of each layer using Marc Mentat software.

The material properties for each CEP layer of the FE IVD model defining the composition gradient had to be calculated. An interpolation of the experimental results of the distribution of components through the disc from Roberts et al. [7] and the values of the parameters from the FE IVD model from Ruiz Wills et al. [10] was made. A equation, linear or parabolic, was defined for each component and degeneration degree (Table 2).

		GRADE I	GRADE III
Initial water content (% of wet weight)		$y = 52 + 34{,}5679x$	$y = 44 + 39{,}50617x$
Fixed charge density (mEq/mL)		$y = 0{,}04 + 0{,}32098x$	$y = 0{,}03 + 0{,}246913x$
Collagen content (% of dry weight)	**1st section**	$y = 24 - 35{,}42447(x - 0{,}405)^2$	$y = 35 - 35{,}5938(x - 0{,}405)^2$
	2nd section	$y = 24 - 54{,}87(x - 0{,}405)^2$	$y = 35 - 39{,}6284(x - 0{,}405)^2$

Table 2. Equations of CEP material parameters

The equation approximately represented the shape of the main extracellular matrix constituents distribution function of the graph of Roberts et al. [7], fitted to the values of Ruiz Wills' model [10]. As shown in Table 1, linear equations were calculated for water and fixed charge density content. For collagen content, two parabolic equations were defined, one for the first part of the function till the top point, and other equation for the rest of the function. The value of each component depends on the distance (in mm) from the BEP to the Nucleus, which is the "*x*" factor of the equation. A graphical comparison of the developed equations and the measurements made in [7] for Grade I is shown in Figure 6

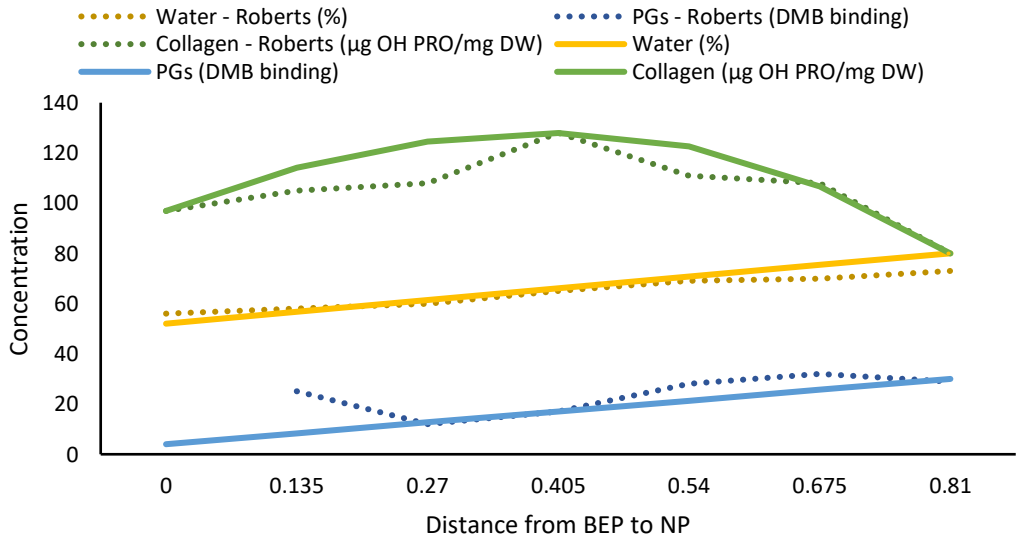

Figure 6. Comparison between experimental measurements from Roberts [8] and the developed equations for each component

Furthermore, the CEP followed a composition-dependent permeability formulation (Equation 10), developed by Ruiz Wills [10] , which depended on the proteoglycan fixed charge density (C_F), collagen content ($\rho_{c,tot}$) and the total water content (n_F). For its calculation, the initial water content of each layer of the IVD model with CEP composition gradient was used.

$$\kappa_{CEP} = A \cdot exp\left(B \cdot c_F + C \cdot \rho_{c,tot}\right) \cdot \left(\frac{1-n_{F0}}{1-n_F}\right)^M \qquad (10)$$

3.3 Boundary conditions

Three different types of FE IVD models were used to perform the simulations. The first type of IVD model was the control one. It was the generic IVD model with constant composition of the CEP used in [10]. The second one was an IVD model who considered a composition gradient of the CEP in its two layers of elements. The third type was an IVD model who considered a composition gradient of the CEP in four layers of elements, so changes were made in the mesh model as explained in Section 3.2.

Each FE IVD model was considered in two different conditions: having Grade I and Grade III according to Pfirrmann grading Scale. Thus, a total of six 3D FE IVD models were evaluated through mechano-transport simulations.

For the mechanical simulations, the activity of a day cycle was simulated involving 8 hours of rest under a compression load of 0,11MPa and 16 hours of activity under a compression load of 0,54MPa, which is the mean load a human supports on a day [23]. This load was applied to the upper Bony Endplate while the lower Bony Endplate was fixed. Disc was considered pressurized. A pre-step of 17 hours of Free Swelling was considered before starting the day cycle simulation to stabilize the internal loads of the disc. The parameters evaluated were fluid velocity, fluid mass transported or mass flow, calculated as the integration of the fluid velocity along time and water content. It was evaluated at the nodes shown in Figure 7.

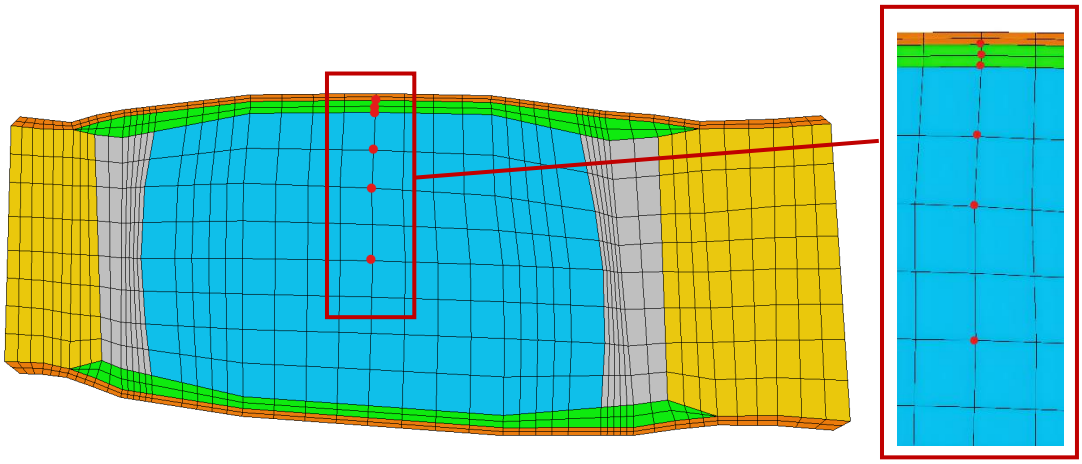

Figure 7. Points of evaluation of mechanical simulations

For transport simulations three daily cycles were simulated, as in [24] was observed that it is enough to start to observe cell death. A previously initialized model for each solute (oxygen, lactate and glucose) was used and in the case of the control IVD model, a previously initialized IVD model. For the other two IVD models, the initialized models for each solute and the routines formulation had to be modified to correlate with the IVD models (see 8.3 from Additional Information). Also the initialization of the IVD models had to be made.

The parameters evaluated from transport simulations were oxygen, lactate and glucose content, water content and cell viability. The pH was also studied through Equation 7, which relates lactate content to pH. These were evaluated in the points shown in Figure 8. The first point of evaluation is located in the Posterior Transition Zone, as it is the thinner part of the disc. This is the region where there is a higher probability for suffering from disc herniation. The second one is at the center of the Nucleus. This is the most disadvantaged region in terms of nutrition. The third node of evaluation is the Anterior Transition Zone. This is the region that supports more loads. It has higher cell activity and higher tissue consolidation. Transport simulations were not run on the IVD model with the 4-layer composition gradient due to a lack of resources on the server.

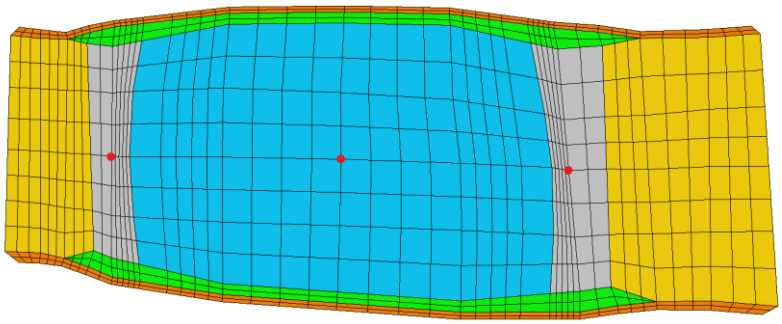

Figure 8. Points of evaluation of transport simulations

4. RESULTS

4.1 Definition of the CEP composition gradient

The result of the division of the CEP element layers to define the CEP 4-layer composition gradient IVD model is shown in Figure 9. The layers were labeled as CEP-Z1 to CEP-Z4 depending on its closeness to the NP, being CEP-Z1 the closest layer to it. On Table 3, it can be shown the difference in element and node number between the generic model and the CEP 4-layer composition gradient IVD model.

	Elements	**Nodes**
Generic IVD model	17088	57379
CEP 4-layer composition gradient IVD model	19680	67979

Table 3. Elements and node number of the FE IVD models

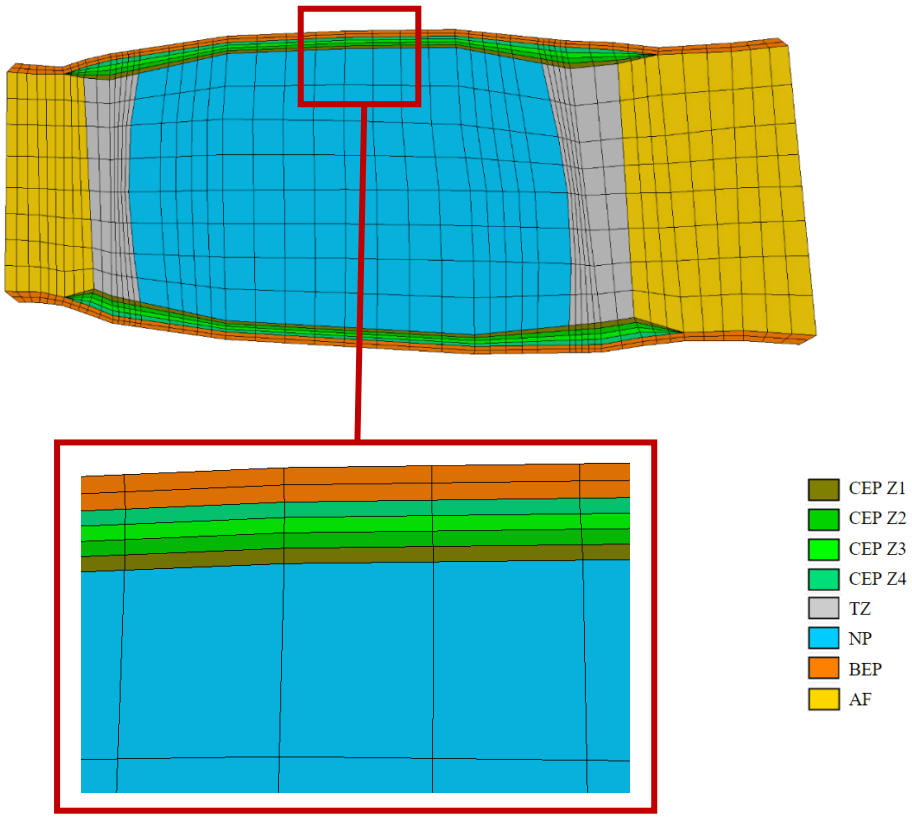

Figure 9. Four-layer CEP IVD model

The material parameters for each CEP element layer were calculated using the equations from Table 2 and Equation 7. They are shown in Table 4 together with permeability and void ratio values. Considering that the generic model had a mean thickness of 0,81 mm, the distances considered were 0 mm for the values associated to CEP-Z4, 0,2025 mm for the values associated to CEP-Z3, 0,405 mm for the values associated to CEP-Z2 and 0,6075 mm for the values associated to CEP-Z1. In the case of the IVD model with a 2-layer CEP composition gradient, the values calculated for CEP-Z4 and CEP-Z2 of the previous model were considered.

	CEP Z1		**CEP Z2**		**CEP Z3**		**CEP Z4**	
	Grade I	**Grade III**	**Grade I**	**Grade III**	**Grade I**	**Grade III**	**Grade I**	**Grade III**
Initial Water Content (%)	73	68	66	60	59	52	52	44
Initial Fixed Charge Density (mEq/ml)	0,235	0,18	0,17	0,13	0,105	0,08	0,04	0,03
Collagen Density (%)	20	32,11	24	35	22,55	33,95	18,19	30,802
Permeability	0,0040135	0,01421	0,01788	0,04486	0,0797	0,141613	0,3552	0,447
Void Ratio	2,7037	2,125	1,0411	1,5	1,439	1,08333	1,083	0,78571

Table 4.Material properties of each CEP element layer of the composition gradient

4.2 Simulation results

4.2.1. Mechanical simulation results

Fluid velocity at the node at the boundary between the CEP and NP for Grade I is shown in Figure 10. Results show that fluid velocity through the endplates decreases when considering the CEP composition gradient compared to the control model. Although the magnitude of the value of fluid velocity of the 4-layer CEP composition gradient model does not correlate with the values of the other two models, it can be seen that the shape of the function is similar to the one of the IVD model with the 2-layer CEP composition gradient.

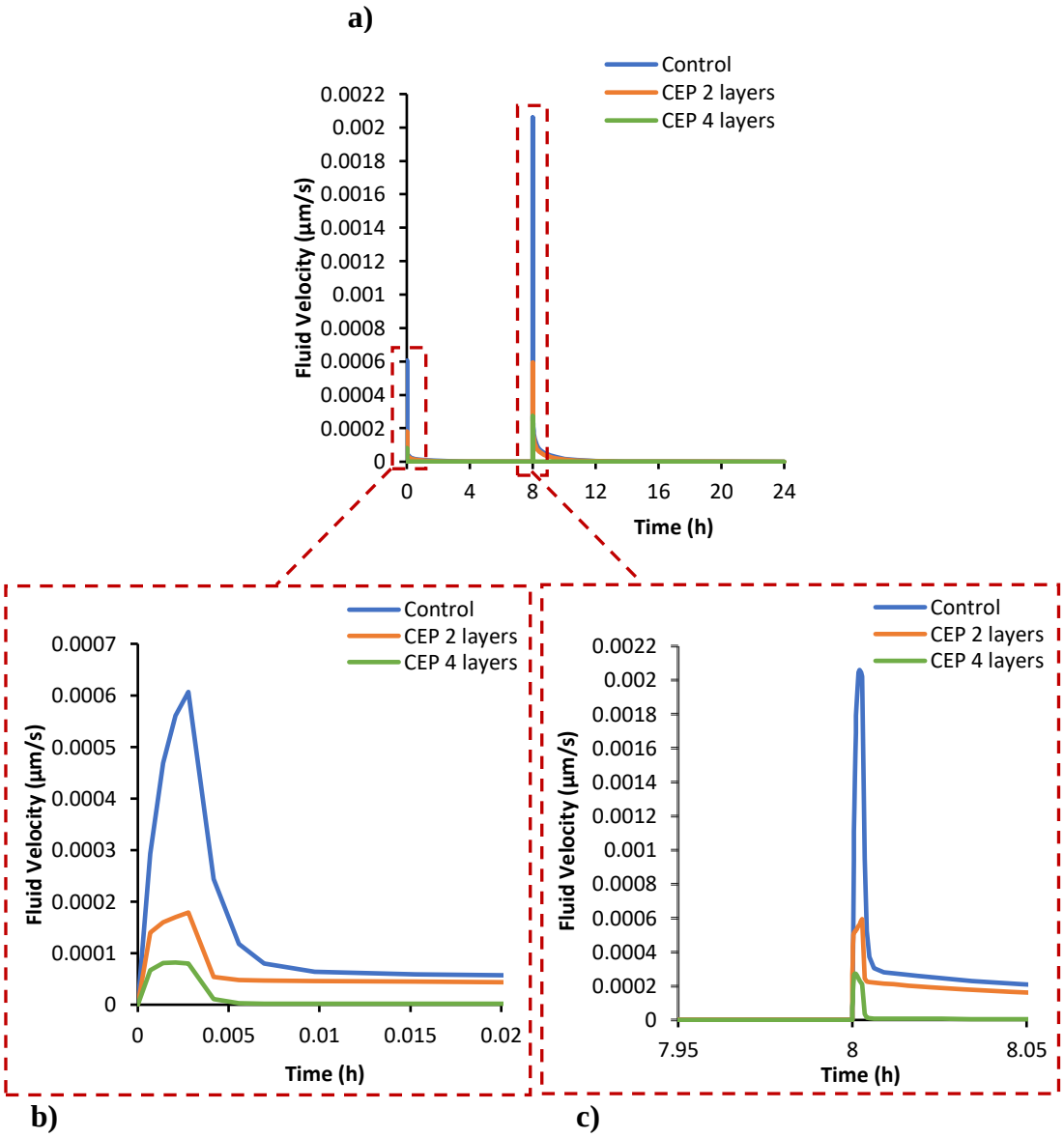

Figure 10. a) Fluid velocity at the boundary CEP-NP for Grade I; b) Zoom at the start of the simulation; c) Zoom at the point of applying the second load (daily activity load).

Figure 11 represents fluid velocity at node at the boundary between the CEP and NP for Grade III. It can be appreciated a large decrease in fluid velocity for the control model compared to the results of Grade I, while in the IVD models with composition gradient there is an increase on fluid velocity.

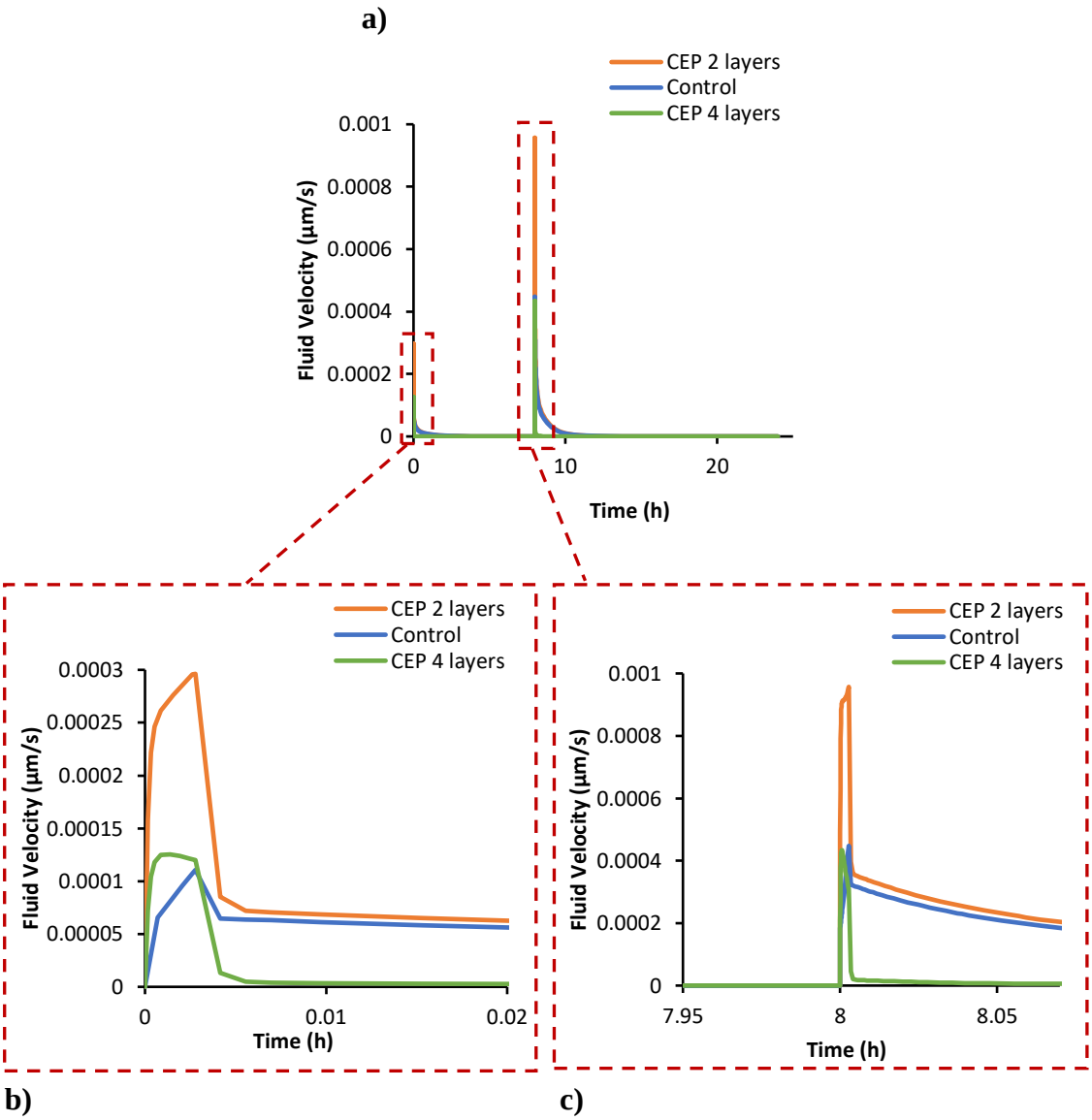

Figure 11. a) Fluid velocity at the boundary CEP-NP for Grade I; b) Zoom at the start of the simulation; c) Zoom at the point of applying the second load (daily activity load)

Mass flow at the boundary between the CEP and NP for Grade I and Grade III can be observed in Figure 12. The control model transports 24.60% more mass flow than the IVD model with the 2-layer CEP composition gradient on Grade I, while it is 11.97% more on Grade III. The IVD model with the 4-layer composition gradient shows very low values of mass flow.

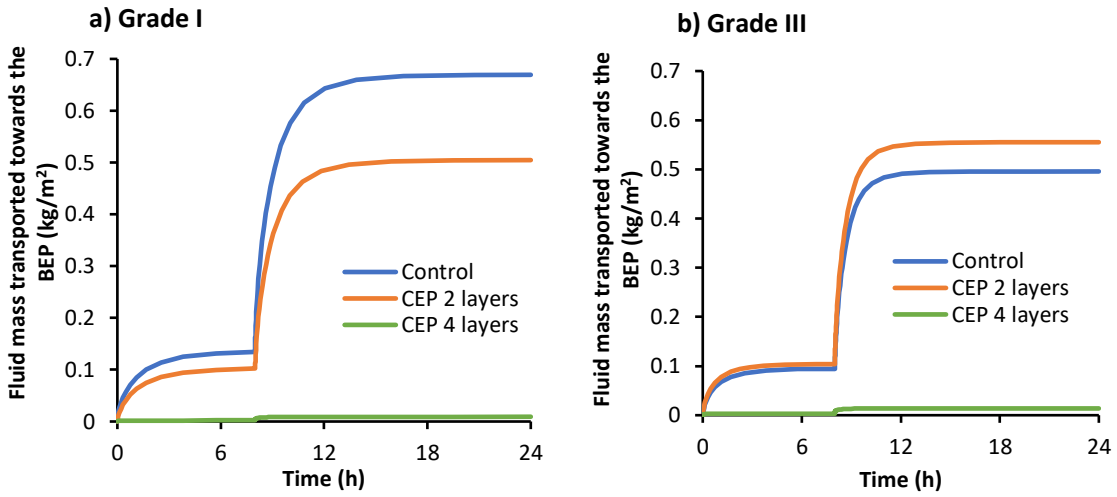

Figure 12. Mass Flow at the Boundary CEP – NP for Grade I and Grade III

Figure 13 compares the results of mass flow at all points of evaluation for the different CEP conditions with Grade I. On the IVD model with the 2-layer CEP composition gradient it can be seen that at the CEP center there is the highest difference to the control IVD model. At the boundary between the CEP and NP, mass flow decreases, while it returns to increase at the first NP node after the CEP and it returns to decrease at the NP center. Furthermore, this graph helps in the identification of the key nodes to study the mechanical results.

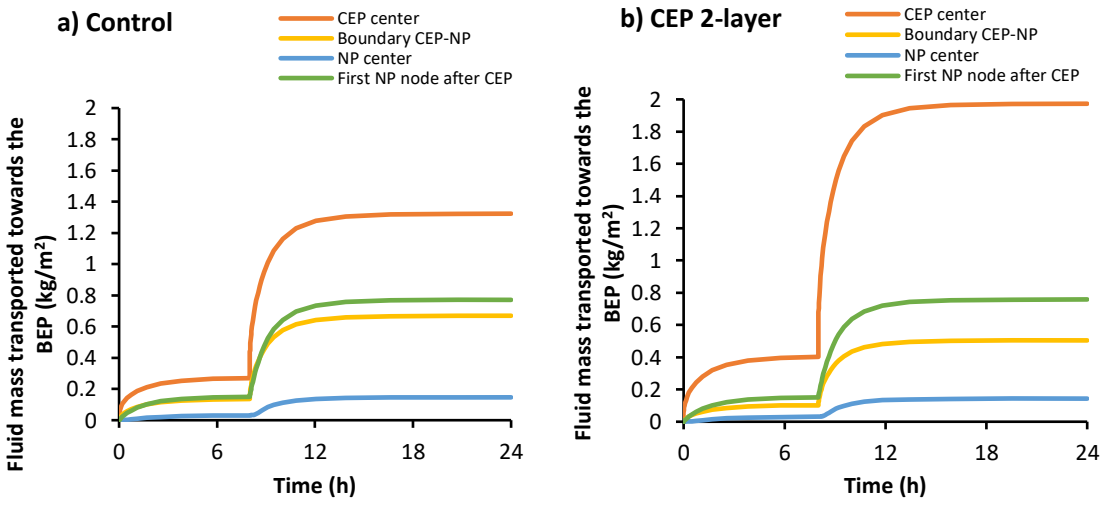

Figure 13. Mass flow on Grade I on a) Control model and b) CEP 2-layer composition gradient model

Water content (porosity) slightly varies between IVD models, as shown in Figure 14. As expected, there is a highest water content on the IVD models with Grade I. In addition, the highest water content is at the NP center in both conditions.

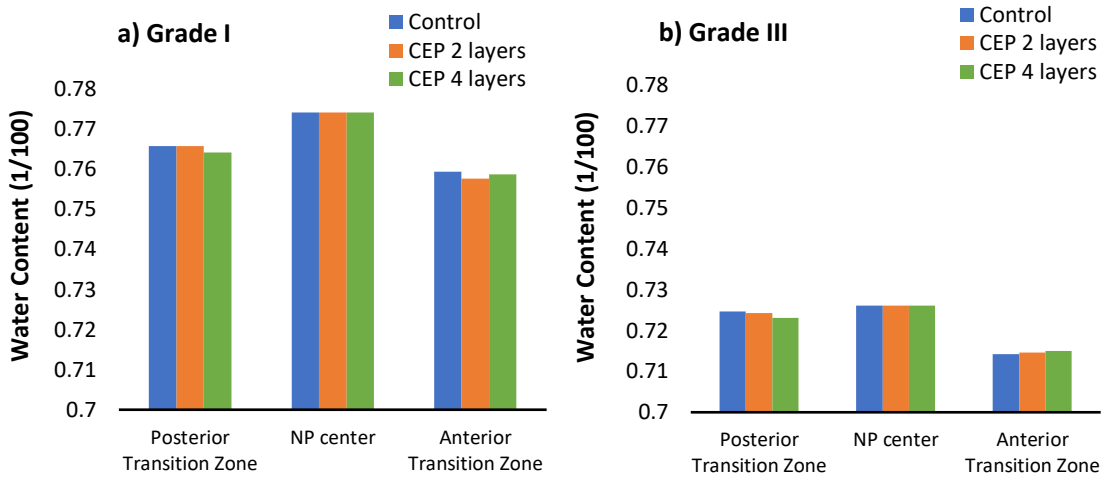

Figure 14. Water content after the daily cycle of mechanical simulation a) Grade I and b) Grade III

At the same time, disc height reduction was calculated by doing the difference of height between the time just after the end of the free swelling step, when all the internal pressures are in equilibrium, and the time at the end of the day of mechanical simulation. It was observed a reduction of 11% of disc height on the control IVD model with Grade I, while on the IVD models with CEP composition gradient it was reduced 11.19%. For Grade III, disc height of the three IVD models was reduced 13%.

4.2.2. Transport simulation results

Transport simulations for the IVD model with 4-layer CEP composition could not be performed due to lack of server resources and disc space. Only the results of the control model and the 2-layer CEP composition gradient IVD model are presented in this section.

The difference on oxygen concentration between the three points of evaluation after three day of simulation is shown in Figure 15. It can be seen that there is lower oxygen concentration in the CEP 2-layer composition gradient IVD model at all points on both degeneration grades. At the NP center there is a greater difference between models. This difference in percentage is of 15.5% on Grade I, while on Grade III it is of 19.58%.

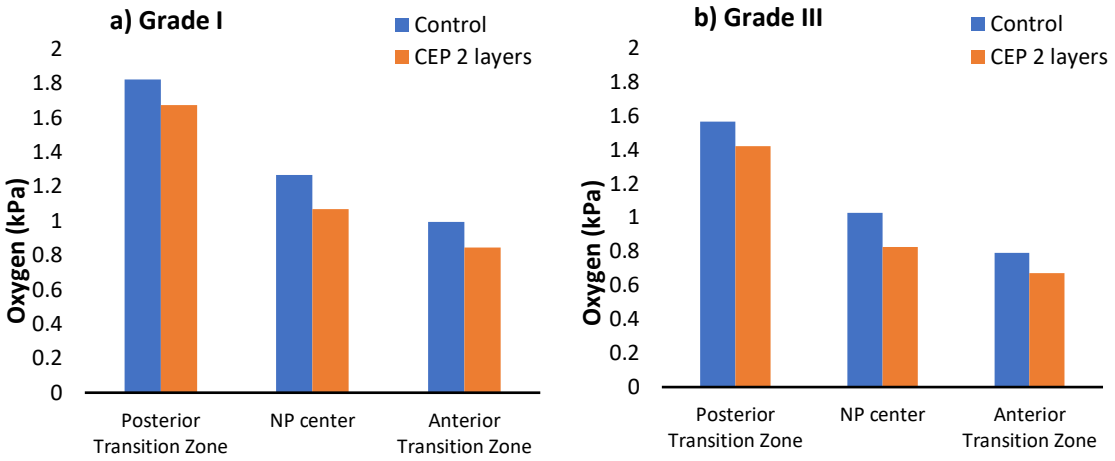

Figure 15. Oxygen concentration at three points on the sagittal path on a) Grade I and b) Grade III after three days of simulation

Lactate concentration after three days of simulation is observed in Figure 16. Contrary to the other solutes, lactate concentration increases from the posterior to the anterior part of the IVD and also with degeneration. Besides, considering the gradient of composition there is an increase on concentration. Otherwise, on the Posterior Transition lactate slightly changes in concentration between grades of degeneration, whereas on the NP center and Anterior Transition Zone there is a greater difference between these two conditions.

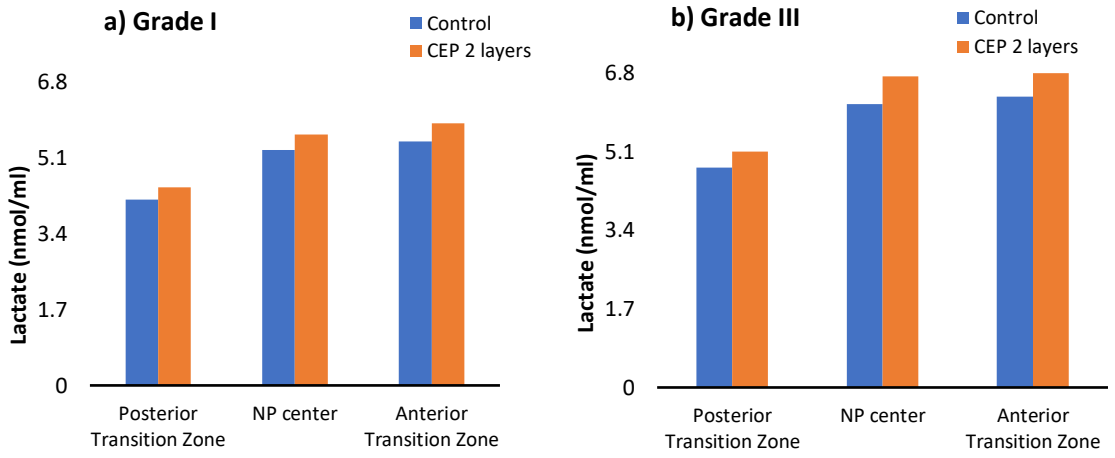

Figure 16. Lactate concentration at three points on the sagittal path on a) Grade I and b) Grade III after three days of simulation

Figure 17 shows the pH values after the three days of simulation at the three evaluation points. It can be seen that in both IVD models the pH values are smaller on Grade III than on Grade I. The red dotted line at a pH value of 6.78 represents the critical value under which cell death is likely to happen. It can be seen that both the NP center and Posterior

Transition Zone are close to this value on Grade III. Moreover, pH levels on the NP center and Anterior Transition Zone are quite similar, compared to the Posterior Transition Zone.

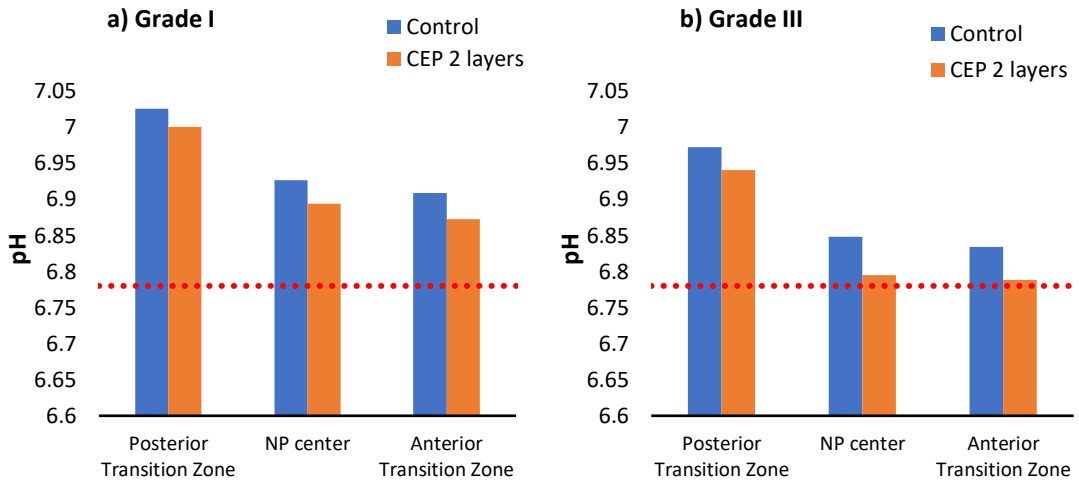

Figure 17. pH at three points of the sagittal path on a) Grade I and b) Grade III after three days of simulation

The results, both on Grade I and Grade III, show a decrease in glucose concentration within the IVD on the model with the 2-layer CEP composition gradient (Figure 18). At the same time, glucose concentration is higher in the IVD models with Grade I. A red dotted line was added to the graph representing critical glucose concentration for cell spread, which is 0.5nmol/mm^3. As seen in the figure, this critical value is reached by the cells at the Anterior Transition Zone of the Grade III models.

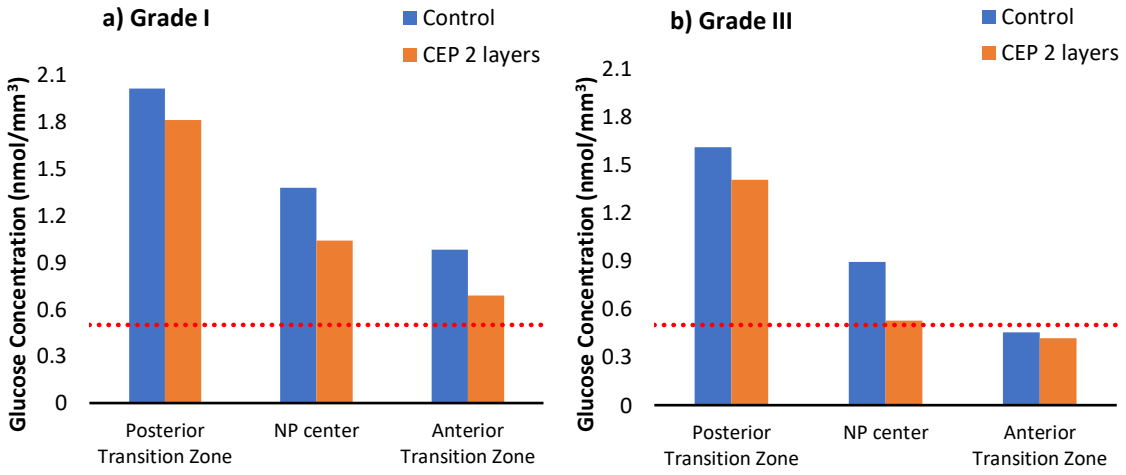

Figure 18. Glucose concentration on a) Grade I and b) Grade III

Cell viability was maintained with a value of 1 for Grade I. In the case of Grade III (Figure 19), it can be seen that the relative cell viability decreases in both models, having a more prominent decrease the IVD model with the CEP 2-layer composition gradient.

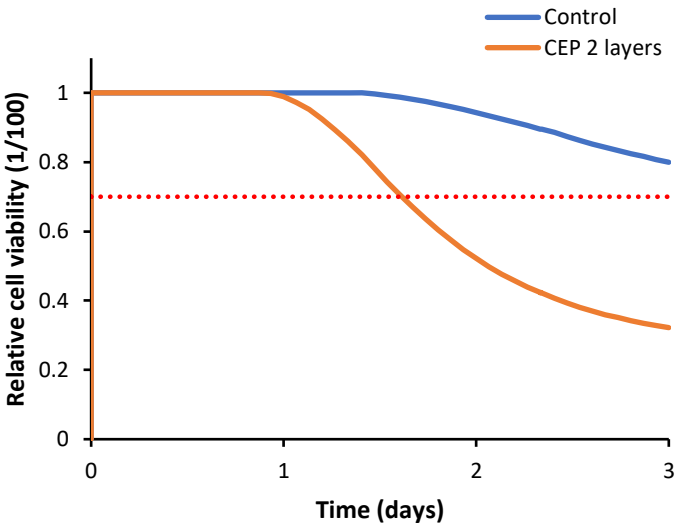

Figure 19. Cell viability at Anterior Transition Zone on Grade III

5. DISCUSSION

A gradient of composition on the cartilage endplates was included in a 3D FE IVD model to explore its influence on disc degeneration. Nutrient solutes were evaluated in different points of the sagittal path for Grade I and Grade III discs. Fluid velocity and mass flow were also evaluated in different points of the vertical path.

As demonstrated by Roberts [7], the cartilage endplates change in composition through the structure. The equations defining each CEP composition parameter developed in this work (water, proteoglycan fixed charge density and collagen) reproduce the experimental measurements made by Roberts [7], as shown in Figure 5.

A larger reduction on disc height was observed on the IVD models with Grade III, compared to the IVD models with Grade I. Degenerated discs are known to have more water loss, resulting in a more fibrotic tissue. Hence, the disc has a lower recovery capacity against the application of loads, decreasing tissue consolidation. Besides, the IVD models with CEP composition gradient with Grade I suffered a little larger disc height reduction than the control IVD model. This difference is due to the CEP properties. The presence of the composition gradient softens the change of material properties at the boundaries between the BEP-CEP and CEP-NP. This helps the tissue to deform when supporting a mechanical load being able to deform a little more, until it consolidates.

Comparing fluid velocity between healthy and degenerated discs, a general decrease on fluid velocity in the degenerated models was observed. Focusing on the different CEP conditions, results suggest that the composition gradient slows down water flow when loads are applied to the disc. The 2-layer CEP composition gradient on Grade I reduced by 71% the maximum fluid velocity at the boundary between the CEP and NP, compared to the control model. This results agree with Ruiz Wills study [10] where a 2D IVD model

with CEP permeability gradient reported similar outcomes, the maximum fluid velocity was reduced by around 50%. Nevertheless, he just simulated a representative loading and unloading cycle. In this project, where the first 3D IVD model with CEP composition gradient was developed, the results showed that with a physiological daily load on a 3D IVD model the composition gradient of the CEP also attenuates fluid velocity.

From the graphs representing mass flow at all evaluation points of mechanical simulation, differences on mass flow were observed when including the gradient of composition. In general, the composition gradient allows greater exchange of water through the cartilage endplate being able to affect nutrient transport. Also, at the node of the boundary between the CEP and NP it is seen that mass flow increases with degeneration. Roberts [13] experimental results agree with the ones obtained, she demonstrated that degenerated discs had more mass flow. This happens because there is less proteoglycan content on the CEP matrix on degenerated discs, which widens the diffusion channels allowing more mass exchange. Because of this, the boundary between the CEP and NP is identified as the key point as it provides more useful information about the mechanical behavior of the disc.

The calculated fluid mass transported towards the BEP or fluid flow reflected an increase in the degenerated IVD model respect to the healthy IVDs with CEP composition gradient, while the opposite happened in the control model. The increment in fluid flow represents that a larger amount of substances diffuse through the CEP, there is a high mass exchange meaning that many substances are lost. This condition does not benefit IVD mechanics.

As shown in Figure 12, the composition gradient does not have a significant effect on mass flow within the NP. In the case of the CEP center, mass flow is much higher on the IVD model with CEP composition gradient. Although it happens the contrary at the boundary between the CEP and NP.

Water content results suggest that it is not much influenced by the CEP composition gradient after the daily cycle of simulation. Despite this, a decrease in water content is seen on degenerated discs compared to healthy discs. These results are similar to the ones obtained by Ruiz Wills [10]. Besides, the Anterior Transition Zone is the disc region with the lowest water content because there is more consolidation. This suggests that degeneration produces NP and TZ dehydration. The effect of this reduction on water content due to degeneration is related to the loss of solute concentrations. This condition does not benefit mechanically because water content contributes to the equilibrium of the osmotic pressure within the NP, which helps in the compressive loads support.

In the case of solutes concentration (oxygen, lactate and glucose), the results suggest that the gradient of composition has an effect on them. In general, lower concentrations were obtained on the IVD models with CEP composition gradient and also on degenerated IVD models. This agrees with Shankar [25], who stated that degenerated discs have a decreased diffusion rate as compared with healthy discs. In addition to this, Anterior Transition Zone is the region that suffered more changes in concentration and where these changes are more critical for disc health.

Gradient of composition reduced oxygen concentration by a 20%. Even though such reduction might have not influenced the cells at the tissue level, its influence in a lower level needs to be further explored. By its part, lactate concentration has the opposite behavior than the rest of solutes on the sagittal path. The increase in lactate concentration within the disc on Grade III occurs because the lactate exit mechanism fails and it accrues within the disc. Urban et al [5] also observed an opposite behavior of lactate than oxygen and glucose on the vertical axis.

Focusing on pH, healthy discs maintained a pH value between 6.87 and 7.02. Under the condition of disc degeneration, the NP center and Anterior Transition Zone were more affected. Cell environment became more acid at the anterior TZ when the gradient was considered. In fact, pH levels decreased almost to activate cell death. This could confirm that it is important to consider the composition gradient as it could represent critical values that determine cell viability and disc health and which cannot be reflected in the control CEP IVD model. Such model might be missing some important data and information.

Glucose is the solute that varies more in composition both at the different points of the sagittal path and between grades. Also, the difference between the control and the IVD model with composition gradient is higher at the NP center. Glucose suffers an abrupt decrease in composition at the Anterior Transition Zone on Grade III, reaching critical values and thus, inducing cell death. Moreover, critical values were almost obtained at the NP center on the degenerated model with composition gradient. This decrease in glucose concentration could be because its transport through the CEP is affected. Degeneration of the IVD hinders the diffusion of glucose through the CEP, so that not enough glucose goes into the disc.

Cell viability depends on the balance between factors regulating supply of nutrients and those regulating cellular demand [5]. In our case, cell death was activated at the Anterior Transition Zone on both degenerated IVD models. This result was expected just analyzing glucose concentration and pH in this condition, as critical values of both parameters were reached after three days of simulation. Besides, the IVD model with composition gradient presented greater cell death. This could be explained because the Anterior Transition Zone has been reported as a high cell activity region, so if the number of cells alive decrease, there might be some risk to maintain homeostasis and therefore, catabolic processes might be activated affecting the maintenance of the extracellular matrix. This result agrees with Malandrino study [9], who observed that cell viability was affected when having a reduced nutrient supply at the endplates, interacting with tissue deformation after compressive daily cycles. Urban et al [5] also concluded that the CEP could also be responsible for falling nutrient concentration throughout the disc to critical low levels if the CEP becomes blocked. Nevertheless, this fact could be further explored through experimental studies.

Despite the interesting outcomes obtained, there are still some important limitations. Firstly, transport simulations of the IVD model with the 4-layer CEP composition gradient could not be performed. This simulation could be useful to have a more complete view of the CEP composition gradient influence on IVD degeneration. Nevertheless, its effects could be appreciated on the IVD model with the 2-layer CEP composition gradient which represents a good starting point. Secondly, this work was performed on a generic 3D FE IVD model. Using patient-specific IVD model would suppose to have a better

overview of how changes on thickness of a CEP with composition gradient would affect the disc behavior. However, a generic IVD model represents a good beginning to study the effect of the gradient on a 3D model. Thirdly, only Grade I and Grade II was considered. Including more degeneration grades would give further insight about the effect of changing from a healthy disc to a full degenerated disc. Fourthly, it would be needed to performed more simulations to be able to extrapolate the results. Fifthly, experimental studies are needed to validate the results obtained.

6. CONCLUSION

In the present study we do a first step towards the implementation of the CEP composition gradient on 3D FE IVD models, with the aim of better understand IVD biomechanics and biochemistry, IVD nutrition and IVD degeneration. Our results suggest that the CEP composition gradient has significant effects on mass exchange and solute transport through the CEP, particularly glucose. This points out that it is highly relevant to include the composition gradient if it is wanted to get a good grasp of what happens on a nutritional level and its possible effects on disc cells. All in all, this numerical model might be a powerful tool for clinicians to better comprehend IVD degeneration; helping in the development of new treatment strategies to improve the quality of life of patients suffering from low back pain.

7. FUTURE WORK

This work can be considered as the starting point for new studies and developments. The composition gradient of the CEP could be implemented on a patient-specific IVD model to know more precisely what happens on the IVD. For this to be possible, several points should be contemplated. The formulation of the materials of each IVD region would have to be redefined because it is the only formulation developed for numerical IVD models and it has been used since many years. For this to be possible, the redefinition should be accompanied by experimental studies focusing on the CEP composition gradient role on the intervertebral disc. Moreover, all degrees of degeneration should be considered. This way, more specific experimental measurements are proposed to allow the development of a strong accurate 3D FE IVD model.

BIBLIOGRAPHY

[1] "The Global Burden of Low Back Pain - International Association for the Study of Pain (IASP)." https://www.iasp-pain.org/resources/fact-sheets/the-global-burden-of-low-back-pain/ (accessed Jun. 07, 2022).

[2] K. Luoma, H. Riihimäki, R. Luukkonen, R. Raininko, E. Viikari-Juntura, and A. Lamminen, "Low Back Pain in Relation to Lumbar Disc Degeneration," *Spine (Phila Pa 1976)*, vol. 25, no. 4, pp. 487–492, Feb. 2000, doi: 10.1097/00007632-200002150-00016.

[3] "Degenerative Disc Disease Treatment for Low Back Pain." https://www.spine-health.com/conditions/degenerative-disc-disease/degenerative-disc-disease-treatment-low-back-pain (accessed Jun. 07, 2022).

[4] C. M. de Geer, "Intervertebral Disk Nutrients and Transport Mechanisms in Relation to Disk Degeneration: A Narrative Literature Review," *Journal of Chiropractic Medicine*, vol. 17, no. 2, pp. 97–105, Jun. 2018, doi: 10.1016/j.jcm.2017.11.006.

[5] J. P. G. Urban, S. Smith, and J. C. T. Fairbank, "Nutrition of the Intervertebral Disc," *Spine (Phila Pa 1976)*, vol. 29, no. 23, pp. 2700–2709, Dec. 2004, doi: 10.1097/01.brs.0000146499.97948.52.

[6] J. F. DeLucca, D. H. Cortes, N. T. Jacobs, E. J. Vresilovic, R. L. Duncan, and D. M. Elliott, "Human cartilage endplate permeability varies with degeneration and intervertebral disc site," *Journal of Biomechanics*, vol. 49, no. 4, pp. 550–557, Feb. 2016, doi: 10.1016/j.jbiomech.2016.01.007.

[7] S. ROBERTS, J. MENAGE, and J. P. G. URBAN, "Biochemical and Structural Properties of the Cartilage End-Plate and its Relation to the Intervertebral Disc," *Spine (Phila Pa 1976)*, vol. 14, no. 2, pp. 166–174, Feb. 1989, doi: 10.1097/00007632-198902000-00005.

[8] L. Wang *et al.*, "Evaluation of human cartilage endplate composition using MRI: Spatial variation, association with adjacent disc degeneration, and in vivo repeatability," *Journal of Orthopaedic Research*, vol. 39, no. 7, pp. 1470–1478, Jul. 2021, doi: 10.1002/jor.24787.

[9] A. Malandrino, J. Noailly, and D. Lacroix, "Numerical exploration of the combined effect of nutrient supply, tissue condition and deformation in the intervertebral disc," *Journal of Biomechanics*, vol. 47, no. 6, pp. 1520–1525, Apr. 2014, doi: 10.1016/j.jbiomech.2014.02.004.

[10] C. Ruiz Wills, B. Foata, M. Á. González Ballester, J. Karppinen, and J. Noailly, "Theoretical Explorations Generate New Hypotheses About the Role of the Cartilage Endplate in Early Intervertebral Disk Degeneration," *Frontiers in Physiology*, vol. 9, Sep. 2018, doi: 10.3389/fphys.2018.01210.

[11] J. Wong *et al.*, "Nutrient supply and nucleus pulposus cell function: effects of the transport properties of the cartilage endplate and potential implications for intradiscal biologic therapy," *Osteoarthritis and Cartilage*, vol. 27, no. 6, pp. 956–964, Jun. 2019, doi: 10.1016/j.joca.2019.01.013.

[12] A. Dolor, S. L. Sampson, A. A. Lazar, J. C. Lotz, F. C. Szoka, and A. J. Fields, "Matrix modification for enhancing the transport properties of the human cartilage endplate to improve disc nutrition," *PLOS ONE*, vol. 14, no. 4, p. e0215218, Apr. 2019, doi: 10.1371/journal.pone.0215218.

[13] S. Roberts, J. P. G. Urban, H. Evans, and S. M. Eisenstein, "Transport Properties of the Human Cartilage Endplate in Relation to Its Composition and Calcification," *Spine (Phila Pa 1976)*, vol. 21, no. 4, pp. 415–420, Feb. 1996, doi: 10.1097/00007632-199602150-00003.

[14] A. Malandrino, J. Noailly, and D. Lacroix, "The Effect of Sustained Compression on Oxygen Metabolic Transport in the Intervertebral Disc Decreases with Degenerative Changes," *PLoS Computational Biology*, vol. 7, no. 8, p. e1002112, Aug. 2011, doi: 10.1371/journal.pcbi.1002112.

[15] S. Stephan, W. Johnson, and S. Roberts, "The influence of nutrient supply and cell density on the growth and survival of intervertebral disc cells in 3D culture," *European Cells and Materials*, vol. 22, pp. 97–108, Sep. 2011, doi: 10.22203/eCM.v022a08.

[16] "Lumbar Spine Anatomy and Pain." https://www.spine-health.com/conditions/spine-anatomy/lumbar-spine-anatomy-and-pain (accessed Jun. 07, 2022).

[17] F. Guilak, H. P. Ting-Beall, A. E. Baer, W. R. Trickey, G. R. Erickson, and L. A. Setton, "Viscoelastic Properties of Intervertebral Disc Cells," *Spine (Phila Pa 1976)*, vol. 24, no. 23, p. 2475, Dec. 1999, doi: 10.1097/00007632-199912010-00009.

[18] T. Grunhagen, G. Wilde, D. M. Soukane, S. A. Shirazi-Adl, and J. P. G. Urban, "Nutrient Supply and Intervertebral Disc Metabolism," *Journal of Bone and Joint Surgery*, vol. 88, no. suppl_2, pp. 30–35, Apr. 2006, doi: 10.2106/JBJS.E.01290.

[19] I. M. Shapiro and M. v. Risbud, "The intervertebral disc: Molecular and structural studies of the disc in health and disease," *The Intervertebral Disc: Molecular and Structural Studies of the Disc in Health and Disease*, pp. 1–446, Jan. 2014, doi: 10.1007/978-3-7091-1535-0.

[20] C. W. A. Pfirrmann, A. Metzdorf, M. Zanetti, J. Hodler, and N. Boos, "Magnetic Resonance Classification of Lumbar Intervertebral Disc Degeneration," *Spine (Phila Pa 1976)*, vol. 26, no. 17, pp. 1873–1878, Sep. 2001, doi: 10.1097/00007632-200109010-00011.

[21] Y. Schroeder *et al.*, "Are disc pressure, stress, and osmolarity affected by intra- and extrafibrillar fluid exchange?," *Journal of Orthopaedic Research*, vol. 25, no. 10, pp. 1317–1324, Jun. 2007, doi: 10.1002/jor.20443.

[22] S. R. S. Bibby, D. A. Jones, R. M. Ripley, and J. P. G. Urban, "Metabolism of the Intervertebral Disc: Effects of Low Levels of Oxygen, Glucose, and pH on Rates of Energy Metabolism of Bovine Nucleus Pulposus Cells," *Spine (Phila Pa 1976)*, vol. 30, no. 5, pp. 487–496, Mar. 2005, doi: 10.1097/01.brs.0000154619.38122.47.

[23] H. Wilke, P. Neef, M. Caimi, T. Hoogland, and L. E. Claes, "New In Vivo Measurements of Pressures in the Intervertebral Disc in Daily Life," *Spine (Phila*

Pa 1976), vol. 24, no. 8, pp. 755–762, Apr. 1999, doi: 10.1097/00007632-199904150-00005.

[24] H. A. Horner and J. P. G. Urban, "2001 Volvo Award Winner in Basic Science Studies: Effect of Nutrient Supply on the Viability of Cells From the Nucleus Pulposus of the Intervertebral Disc," *Spine (Phila Pa 1976)*, vol. 26, no. 23, pp. 2543–2549, Dec. 2001, doi: 10.1097/00007632-200112010-00006.

[25] H. Shankar, J. A. Scarlett, and S. E. Abram, "Anatomy and pathophysiology of intervertebral disc disease," *Techniques in Regional Anesthesia and Pain Management*, vol. 13, no. 2, pp. 67–75, Apr. 2009, doi: 10.1053/j.trap.2009.05.001.

References of Figures

[Figure 1] - Orthoinfo.aaos.org. 2022. *Spine Basics - OrthoInfo - AAOS*. [online] Available at: <https://orthoinfo.aaos.org/en/diseases--conditions/spine-basics/>
[Figure 2] - D3i71xaburhd42.cloudfront.net. 2022. [online] Available at: <https://d3i71xaburhd42.cloudfront.net/ccdcee0a3c16c042c1b4265782db6dea68c663d9/2-Figure1-1.png>

[Figure 3] – Figure 1 from Huang, Y., Urban, J. and Luk, K., 2014. Intervertebral disc regeneration: do nutrients lead the way?. *Nature Reviews Rheumatology*, 10(9), pp.561-566.

[Figure 4] - Operativeneurosurgery.com. 2022. *pfirrmann_grading_system [Operative Neurosurgery]*. [online] Available at: <https://operativeneurosurgery.com/doku.php?id=pfirrmann_grading_system>

[Figure 20]: Figure 2 from A. Malandrino, J. Noailly, and D. Lacroix, "Numerical exploration of the combined effect of nutrient supply, tissue condition and deformation in the intervertebral disc," *Journal of Biomechanics*, vol. 47, no. 6, pp. 1520–1525, Apr. 2014, doi: 10.1016/j.jbiomech.2014.02.004.

8. ADDITIONAL INFORMATION

8.1 BEP and AF collagen fibers material properties

Table 5 and Table 6 show the material properties used on BEP and AF collagen fibers for both Grade I and Grade III.

Young's Modulus	Poisson's Ratio	Permeability	
		K	Void Ratio
10000	0.3	26800	0.05

Table 5. BEP properties

	Dashpot Stiffness [MPa s]	E1 [MPa]	K1 [MPa]	E2 [MPa]	K2 [MPa]
Grade I	4000	2.8	11	6.1	8
Grade III	14000	3.7	18.5	7	14

Table 6. AF collagen fibers properties

8.2 Transport simulation scheme

Figure 20 shows the coupling scheme between poromechanical FE model and transport FE models. They are coupled through porosities and deformation fields which are used to update the gradients of concentration over time. It is a closed loop that by the interaction of the metabolic reactions of oxygen, lactate and glucose, calculates cell viability and the consumption/production of each solute at each time point.

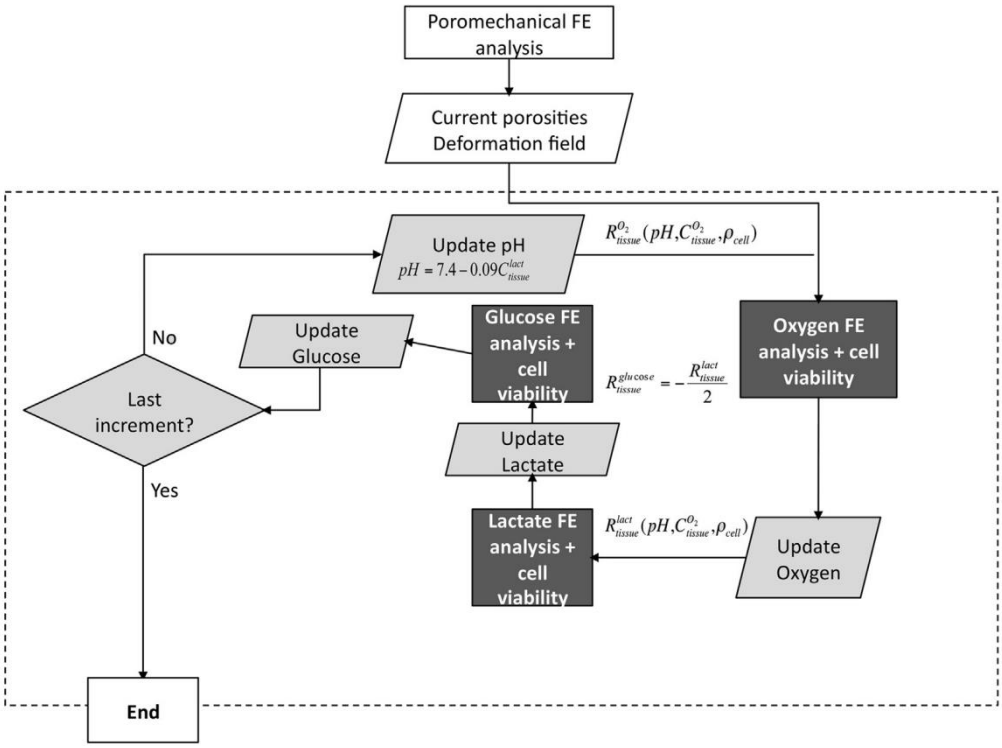

Figure 20. Transport simulation workflow

8.3 Boundary Conditions of transport simulations

The routines of transport simulations had to be modified for the CEP composition gradient IVD models. Particularly, CEP water content and cell density were the parameters modified. Water content values are the same as those of the boundary conditions of mechanical simulation. Table 7 specifies water content values for the 2-layer CEP composition gradient. The control IVD model used the CEP Z2 water content values. Cell density for each CEP layer was calculated splitting cell density value of the control IVD model by two, the number of layers defining the composition gradient. Moreover, cell density is considered the same for Grade I and Grade III. Table 8 specifies cell density values for each IVD model.

	CEP Z2		**CEP Z4**	
	Grade I	**Grade III**	**Grade I**	**Grade III**
Initial Water Content (%)	66	60	52	44

Table 7. CEP initial water content on transport simulations

	Control model	**2-layer CEP composition gradient**	
		CEP Z1	**CEP Z2**
CEP Cell density	0.0135	0.00675	0.00675

Table 8. Cell density for the IVD models